Full-Bridge Rectifier Input Reactance Compensation in Megahertz Wireless Power Transfer Systems

Minfan Fu, Zefan Tang, Ming Liu, Chengbin Ma*, Xinen Zhu
University of Michigan - Shanghai Jiao Tong University Joint Institute
Shanghai, China

***Abstract*—It is attractive to achieve wireless power transfer with large spatial freedom by using a Megahertz system. For most systems, especially those working at kHz, the rectifiers are equivalently modelled as pure resistive loads when designing the compensated capacitors for coupling coils. However, the input reactance occurs when a rectifier works at high frequency, such as Megahertz. It can disturb the original circuit resonance designed without considering this reactance. This paper analyzes the input reactance for the full-bridge rectifier and evaluates its effects on the originally resonant coupling coils. A novel compensation method is proposed to eliminate the input reactance effects. Finally, a 6.78 MHz system is implemented in experiment. It shows that the compensation method can improve the system efficiency from 65% to 84% for the best case.**

Keywords*—Wireless power transfer, full-bridge rectifier, compensation, input reactance, impedance matching

I. INTRODUCTION

Wireless power transfer (WPT) has attracted an ever increasing interest from both industrial and academic sectors over the past years. Based on resonant inductive coupling, it is of high potential to achieve medium-range power transfer [1]. The use of WPT can lead to a revolutionary change for charging electronic devices, such as small sensors, portable devices, household appliances, and even high-power electrical vehicles and trains. A well-performed WPT system usually needs to consider various issues, including power level, efficiency, distance, system stability, EMI, etc. The importance of these issues are different for various applications. For example, a WPT system can be designed to work at kHz for high-power EV charging [2]. In order to ensure the required system power and efficiency, a strong coupling is desired between the coils to enhance the power transfer capability. For consumer devices, it is more attractive to build a WPT system with large spacial freedom, which can even enable the charging of multiple devices [3], [4]. The requirement of large spacial freedom is usually achieved by increasing the system frequency. However, it does not mean the higher frequency the better. Because a high working frequency will increase the circuit design difficulty for the other power transformation blocks in a WPT system, especially the power source and the rectifier. Therefore, most high-frequency WPT applications choose their working frequency at several MHz [5]–[7].

There are many published works for MHz WPT systems, such as high-efficiency power amplifiers [8], automatic impedance matching networks [9], suitable high-efficiency rectifiers [10], and optimal load control [6], [7]. Some of the general analysis, although validated in kHz systems, can also be applied for MHz system, especially the analysis for the coupling coils [11]–[14]. The accurate analysis for the coupling coils is necessary to properly design the compensation capacitors for resonance [15]. When conducting system analysis, the direct load of the receiving coil is the input impedance of the rectifier, which usually uses full-bridge topology. However, in most papers, the input impedance of rectifiers are usually modelled as pure ac resistors [1], [2], [11]–[14]. This assumption is no longer valid for MHz rectification due to the non-neglectable parasitic parameters of the diodes. These parameters directly lead the occurrence of input reactance at the input port of the rectifier. Therefore, when designing compensated capacitors for MHz WPT systems, it is necessary to consider the input reactance of the rectifier.

This paper first carries out a simulation-based analysis for the input impedance of a full-bridge rectifier working at MHz. Then the rectifier input reactance is added into the general analysis for the coupling coils. It compares the system performance with and without the undesirable rectifier input reactance. A novel compensation method is proposed to eliminate the effects of this input reactance and shown to be valid in simulation. In the final experiment, it shows that the proposed compensation method can successfully improve the system efficiency for a wide load range.

II. SYSTEM ANALYSIS

A. Rectifier Input Impedance

For most WPT applications, the full-bridge topology is used for rectification due to its simple structure. As shown in Fig. 1, Z_L and R are the input impedance and direct load of the rectifier. P_{ZL} is the ac power extracted from the receiving coil by the rectifier, and P_R is the dc power after rectification. The rectifier efficiency is

$$\eta_{REC} = \frac{P_R}{P_{ZL}}. \tag{1}$$

In the traditional analysis, the rectifier input impedance Z_L is modelled as a pure resistive load for the receiving coil. However, this assumption is no longer valid for high-frequency rectification. At a high-frequency system, the device parasitic parameters become obvious and make the diode no longer an ideal switch. Usually a high-order circuit model is used to describe diode characteristics as shown in Fig. 1 [16]. These undesirable parameters will introduce non-neglectable imaginary part for Z_L, i.e., input reactance. Therefore, the accurate rectifier input impedance can be defined as follows:

$$Z_L = R_L + jX_L, \tag{2}$$

where R_L is the input resistance and X_L is the input reactance.

978-1-4799-6610-3/15/$31.00 ©2015 IEEE

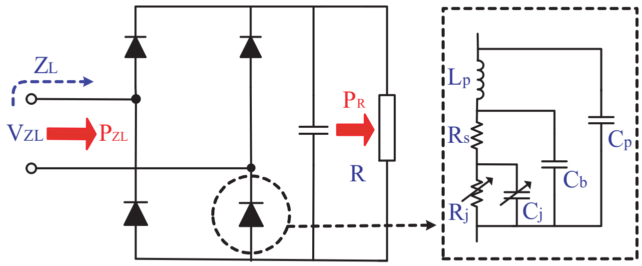

Fig. 1. Full-bridge rectifier topology and high-frequency diode circuit model.

In order to analyze Z_L, a circuit-model-based simulation is carried out in a widely-used RF software ADS. A rectifier is built with the diode spice model (DFLS240L from Diodes Inc. and used in the final experimental system). During the simulation, the rectifier input voltage V_{ZL} is fixed at 20 V and R is varied from 10 Ω to 400 Ω.

Fig. 2 gives the rectifier efficiency for different frequencies. It shows that rectifiers working at low frequency can give a higher efficiency than those working at high frequency, such as 6.78 MHz. Fig. 3 gives the input resistance and reactance for different R. At low frequency (power electronics band), R_L is almost linearly proportional to R, and X_L is negligible compared to R_L. At high frequency (RF band), the relationship between R_L and R becomes more nonlinear and X_L becomes obvious and compatible to the R_L. These results can be well explained by the diode model given in Fig. 1. The switching speed of a diode is one of the most critical parameter, and it is mainly determined by the on-off transient time of the diode. This transient time is caused by the charging and discharging of those shunt capacitors (C_j, C_b and C_p in Fig. 1). At the low frequency, the transient time is much smaller than the switching period. When the diode is on, it can see a resister at the input port (R_j is nearly zero); when the diode is off, it can see an open circuit due to the infinite R_j. Therefore, the input impedance is nearly pure resistive as shown in Fig. 3 (a). As the frequency increases, the transient time will become compatible to the switching period. It means the shunt capacitors behave more like ac components. These shunt capacitors finally contribute to the negative X_L as shown in Fig. 3 (b).

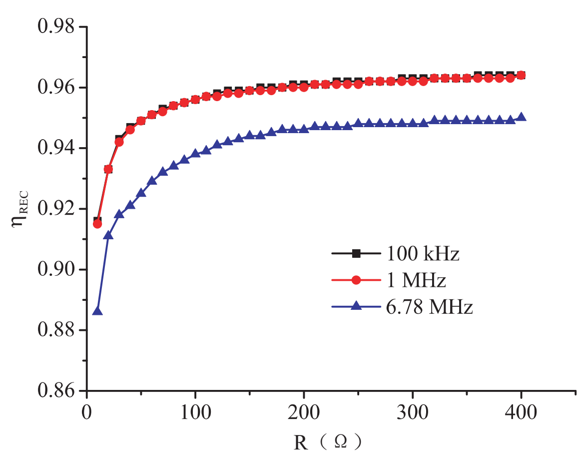

Fig. 2. Rectifier efficiency η_{REC} for different frequencies.

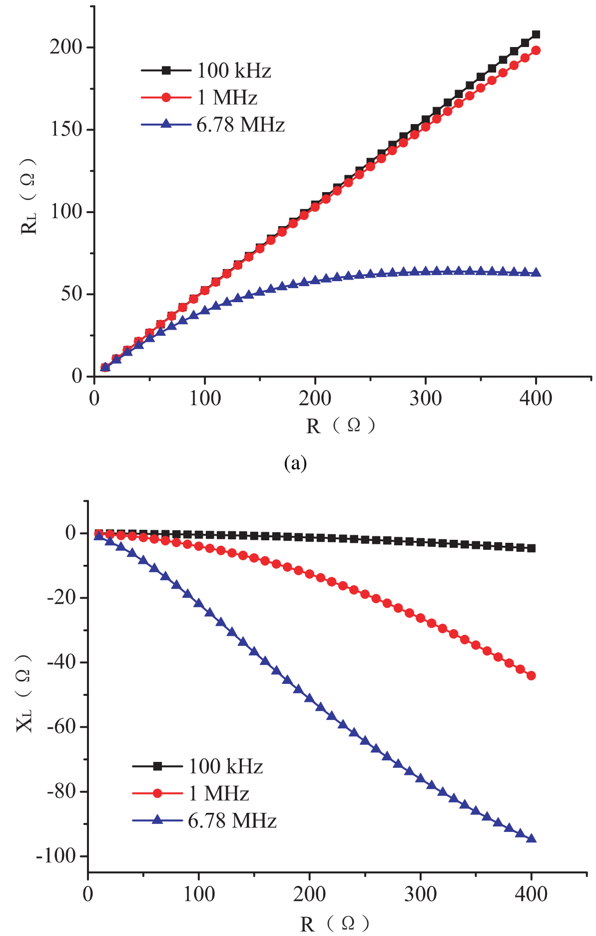

(b)

Fig. 3. Rectifier input impedance Z_L for different frequencies. (a) Input resistance R_L. (b) Input reactance X_L.

B. The Influence of X_L

The influence of X_L can be evaluated by the system as shown in Fig. 4. In this system, the coupling coils (a transmitting coil and a receiving coil) are added for system analysis. L_1, L_2, R_1, R_2 are the self-inductances and self-resistances of the coils. Usually, capacitors C_1 and C_2 are used for coils compensation by

$$j\omega L_i + \frac{1}{j\omega C_i} = 0,\ i = 1\ or\ 2, \tag{3}$$

where ω is the resonance frequency. I_1 and I_2 are the currents of the transmitting coil and receiving coil respectively. The induced voltage due to I_1 for the receiving coil is $j\omega L_M I_1$. And Z_R means the reflected impedance of the receiving side at the transmitting size. Under resonance,

$$Z_R = \frac{\omega^2 {L_M}^2}{R_2 + Z_L}. \tag{4}$$

The input impedance of the coupling coils is

$$Z_{IN} = R_{IN} + jX_{IN} = R_1 + Z_R, \tag{5}$$

where R_{IN} is the coils input resistance and X_{IN} is the coils input reactance. The conversion efficiency of the coupling coils is defined as

$$\eta_{COIL} = \frac{P_{ZL}}{P_{ZIN}}, \tag{6}$$

where P_{ZIN} is the input power of the transmitting coil. This efficiency can also be represented as a product form,

$$\eta_{COIL} = \eta_{TX} \cdot \eta_{RX}, \tag{7}$$

where

$$\begin{cases} \eta_{TX} = \frac{Re[Z_R]}{R_1 + Re[Z_R]} \\ \eta_{RX} = \frac{R_L}{R_2 + R_L} \end{cases} \tag{8}$$

(Re[*] means taking the real part). Thus the overall system efficiency is

$$\eta_{SYS} = \eta_{COIL} \cdot \eta_{REC}. \tag{9}$$

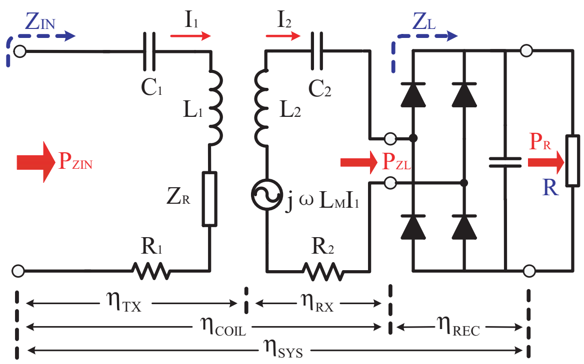

Fig. 4. Circuit configuration.

When Z_L is resistive, i.e., $X_L = 0$, Z_R is pure resistive as below

$$Z_R = Re[Z_R] = \frac{\omega^2 {L_M}^2}{R_2 + R_L}. \tag{10}$$

However, when $X_L < 0$ [refer to Fig. 3 (b)], it has

$$Re[Z_R] = \frac{\omega^2 {L_M}^2}{R_2 + R_L + \frac{{X_L}^2}{R_2 + R_L}}. \tag{11}$$

Compared to (10), $Re[Z_R]$ decreases due to the existence of X_L, leading to an efficiency drop for η_{TX}. Besides, the input impedance Z_{IN} also contains imaginary part due to $Im[Z_R]$ (Im[*] means taking the imaginary part). It has

$$X_{IN} = Im[Z_R] = -\frac{\omega^2 {L_M}^2 X_L}{(R_2 + R_L)^2 + {X_L}^2}. \tag{12}$$

Since $X_L < 0$, Z_{IN} is inductive, which is usually undesirable for the power source.

C. The Compensation for X_L

In order to improve the system performance, it is meaningful to eliminate the input reactance for the transmitting coil, i.e., X_{IN}. A straightforward method is to use impedance matching network to directly compensate X_{IN} at the transmitting side [1], [9]. Since X_{IN} is dependent on R and L_m, the network should provide automatic impedance matching according to load and coil's position variation. Usually this network is achieved by the switching among different capacitors or inductors. Theoretically, both feedback and feed-forward control approaches can be used to tune the network. The feedback method can be achieved by detecting the phase difference between the input current and voltage of the transmitting coil. Then a close-loop control can be applied to ensure a zero phase difference. This method is widely used for kHz WPT application, because there are many mature technologies to support accurate waveform magnitude and phase detection. However, for a MHz system, it is difficult to detect the voltage and current accurately, especially their phase difference. The other control can also be used through a feed-forward method. According to (12), X_{IN} can be completely canceled if L_M and R_L are measured. Thus a open-loop control can be used. However, this open-loop system highly relies on the preciseness of circuit's parameters and hardly satisfies the requirement of robustness. Moreover, it is impractical to detect L_M in real applications.

Instead of introducing impedance matching network at the transmitting side, this paper proposes a method the compensate to reactance at the receiving side. Observing (12), X_{IN} can be zero if $X_L = 0$. It means if X_L is ideally compensated at the receiving side, then Z_{IN} can be pure resistive. This compensation can be achieved by tuning C_2 dynamically instead of using a fixed value defined in (3). The tuning method needs to ensure that L_2, C_2 and X_L together form a resonant circuit as follow:

$$j\omega L_2 + \frac{1}{j\omega C_2} + jX_L = 0. \tag{13}$$

According to Fig. 3 (b), X_L is almost linearly dependant on R. So it can be modelled as

$$X_L = -aR, \tag{14}$$

where a is the slope in Fig. 3 (b). Combining (13) and (14), C_2 can be derived as

$$C_2 = \frac{1}{\omega^2 L_2 - \alpha\omega R} \tag{15}$$

Thus, a open-loop control can be used to tune C_2 according R, which can be easily obtained by measuring the dc voltage and current at the rectifier output port [6].

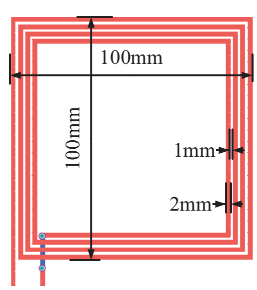

Parameters	Value
Self-Inductance (L_1, L_2)	3.34 (uH)
Self-resistance (R_1, R_2)	0.8 (Ω)
Distance	40 (mm)
Mutual inductance (L_M)	0.55 (uH)

Fig. 5. Coils' layout and parameters.

A simulation is conducted to verify the proposed compensation method. The coils's layout and parameters are shown in Fig. 5. Two square PCB coils are placed face to face with a distance of 40 mm. The circuit of Fig. 4 is built in ADS with a constant ac current source. The RMS value of I_1 is 0.5 A. During the simulation, the original system without compensation [C_2 obtained by (3)] is compared with the system with compensation [C_2 obtained by (15) with $\alpha = 0.3$].

C_1 is fixed at 169 pF and resonates with L_1. Fig. 6 shows the input impedance Z_{IN} for the coupling coils. With the proposed compensation method, the input reactance X_{IN} is controlled to be a small value; the input resistance R_{IN} is improved accordingly. Fig. 7 shows the system efficiency can be improved for a wide range of R.

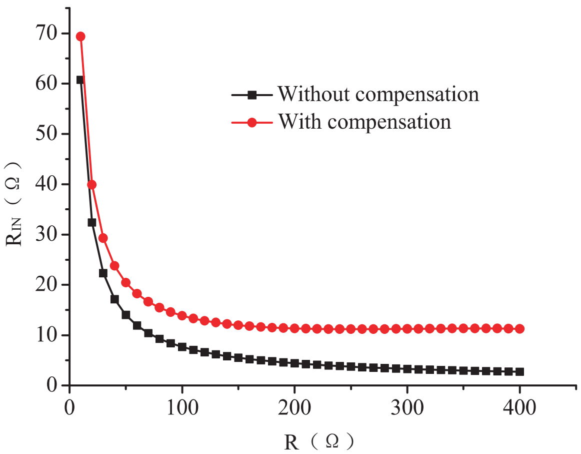

(a)

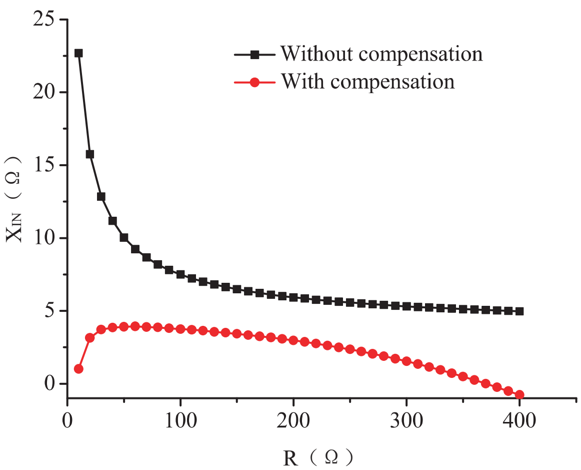

(b)

Fig. 6. The input impedance of the coupling coils Z_{IN}. (a) Input resistance R_{IN}. (b) Input reactance X_{IN}.

III. Experiment

A 6.78 MHz WPT system is built as shown in Fig. 8 for verification. This measurement platform consists of a power amplifier, two coupling coils, a rectifier and an electrical load. The power amplifier can be tuned to provide a constant input current I_1 to drive the coupling coils. For the coupling coils, the setup of experiment is same as that of simulation [refer to Fig. 5]. A full-bridge rectifier is built with four diodes, the same diodes used in Section II-A. The tuning of R can be achieved by the electrical load and the output power of the system can be easily read. The input power P_{ZIN} is obtained by measuring the input voltage and current through oscilloscope. Before the experiment, a pure 50 Ω RF load is directly connected after the power amplifier for calibration. The initial phase delay between the voltage and current probes can be eliminated.

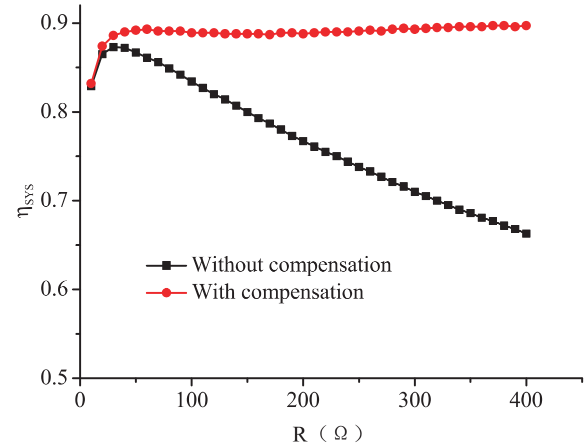

Fig. 7. System efficiency η_{SYS}.

During the experiment, the RMS of I_1 is controlled to be constant at 0.5 A for different R. Fig. 9 shows that the system with compensation can extract more power than the system without compensation. This is because the compensation of X_L can increase R_{IN} as shown in Fig. 6 (a). The system efficiency comparison is given in Fig. 10, which is consistent with the result of Fig. 7. The compensation method has excellent performance for large R. When R = 400 Ω, the efficiency can be drawn back from 65% to 84%.

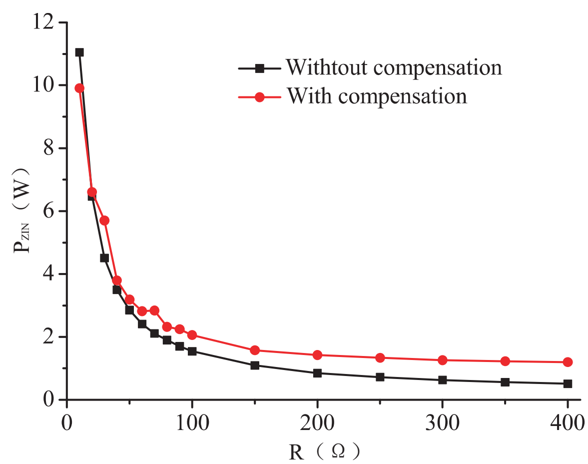

Fig. 9. Input power for different R.

IV. Conclusion

This paper evaluates the input reactance effects of the full-bridge rectifiers for MHz WPT systems. In the simulation, the rectifier input impedance is shown to be capacitive instead of pure resistive for MHz rectification. Then this rectifier input reactance is added into the traditional analysis for the coupling coils. An undesirable input reactance occurs as well at the coupling coils input port and the system efficiency between the coils is shown to be reduced. Based on the rectifier model, a compensation method is proposed to eliminate the rectifier input reactance effects. Finally, an experiment is designed to verify the analysis. The system efficiency can be improved from 65% to 84% for the best case with the compensation method.

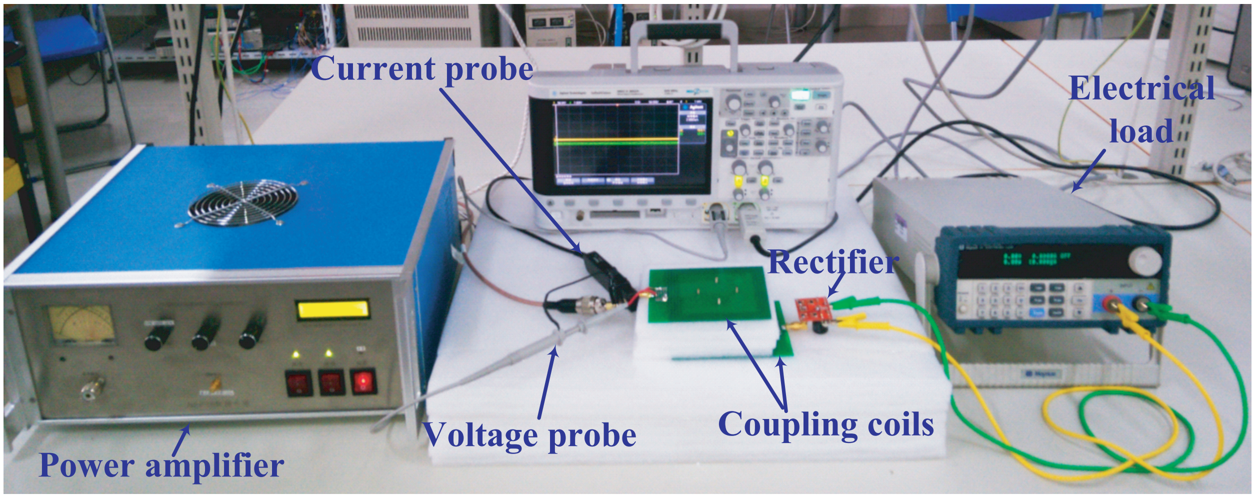

Fig. 8. Experiment setup.

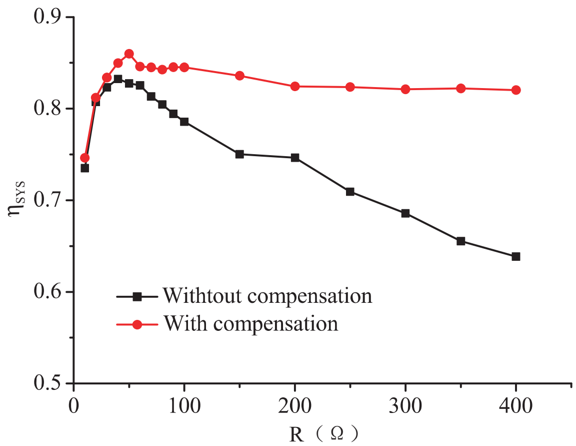

Fig. 10. System efficiency for different R.

References

[1] A. P. Sample, B. H. Waters, S. T. Wisdom, and J. R. Smith, "Enabling seamless wireless power delivery in dynamic environments," *Proc. IEEE*, vol. 101, no. 6, pp. 1343–1358, Apr. 2013.

[2] C.-S. Wang, O. H. Stielau, and G. A. Covic, "Design considerations for a contactless electric vehicle battery charger," *IEEE Trans. Ind. Electron.*, vol. 52, no. 5, pp. 1308–1314, 2005.

[3] D. Ahn and S. Hong, "Effect of coupling between multiple transmitters or multiple receivers on wireless power transfer," *IEEE Trans. Ind. Electron.*, vol. 60, no. 7, pp. 2602–2613, 2013.

[4] T. Zhang, M. Fu, C. Ma, and X. Zhu, "Optimal load analysis for a two-receiver wireless power transfer system," in *Wireless Power Transfer Conference (WPTC), 2014 IEEE*. IEEE, 2014, pp. 84–87.

[5] D. Kurschner and C. Rathge, "Maximizing dc-to-load efficiency for inductive power transfer," *IEEE Trans. Power Electron.*, vol. 28, no. 5, pp. 2437–2447, 2013.

[6] M. Fu, C. Ma, and X. Zhu, "A cascaded boost-buck converter for high efficiency wireless power transfer systems," *IEEE Trans. Ind. Informat.*, vol. 10, no. 3, pp. 1972–1980, 2014.

[7] M. Fu, H. Yin, X. Zhu, and C. Ma, "Analysis and tracking of optimal load in wireless power transfer systems," *IEEE Trans. Power Eletron.*, vol. 30, no. 7, pp. 3952–3963, 2014.

[8] S. Aldhaher, P. C. Luk, and J. F. Whidborne, "Tuning class e inverters applied in inductive links using saturable reactors," *IEEE Trans. Power Electron.*, vol. 29, no. 6, pp. 2969–2978, 2014.

[9] T. C. Beh, M. Kato, T. Imura, S. Oh, and Y. Hori, "Automated impedance matching system for robust wireless power transfer via magnetic resonance coupling," *IEEE Trans. Ind. Electron.*, vol. 60, no. 9, pp. 3689–3698, 2013.

[10] S. Aldhaher, P. Luk, K. E. K. Drissi, and J. Whidborne, "High-input-voltage high-frequency class e rectifiers for resonant inductive links," *IEEE Trans. Power Electron.*, vol. 30, no. 3, pp. 1328 – 1335, 2014.

[11] C. Wang, G. A. Covic, and O. H. Stielau, "Power transfer capability and bifurcation phenomena of loosely coupled inductive power transfer systems," *IEEE Trans. Ind. Electron.*, vol. 51, no. 1, pp. 148–157, 2004.

[12] A. P. Sample, D. A. Meyer, and J. R. Smith, "Analysis, experimental results, and range adaptation of magnetically coupled resonators for wireless power transfer," *IEEE Trans. Ind. Electron.*, vol. 58, no. 2, pp. 544–554, 2011.

[13] L. Chen, S. Liu, Y. C. Zhou, and T. J. Cui, "An optimizable circuit structure for high-efficiency wireless power transfer," *IEEE Trans. Ind. Electron.*, vol. 60, no. 1, pp. 339–349, 2013.

[14] N. A. Keeling, G. A. Covic, and J. T. Boys, "A unity-power-factor IPT pickup for high-power applications," *IEEE Trans. Ind. Electron.*, vol. 57, no. 2, pp. 744–751, 2010.

[15] M. Fu, T. Zhang, C. Ma, and X. Zhu, "Efficiency and optimal loads analysis for multiple-receiver wireless power transfer systems," *IEEE Trans. Microw. Theory Tech.*, vol. 63, no. 3, pp. 801–812, 2015.

[16] J. Hansen and K. Chang, "Diode modeling for rectenna design," in *2011 IEEE International Symposium Antennas and Propagation (APSURSI)*. IEEE, 2011, pp. 1077–1080.

978-1-4799-6610-3/15/$31.00 ©2015 IEEE